PHILOSOPHICAL TRANSACTIONS OF THE ROYAL SOCIETY A MATHEMATICAL, PHYSICAL & ENGINEERING SCIENCES

# The submillimetre extragalactic background light and the star –formation history of the Universe

L. L. Cowie and A. J. Barger

*Phil. Trans. R. Soc. Lond. A* 2000 **358**, 2133-2141
doi: 10.1098/rsta.2000.0635

10.1098/rsta.2000.0635



# The submillimetre extragalactic background light and the star-formation history of the Universe

By L. L. Cowie and A. J. Barger

*Institute for Astronomy, University of Hawaii, 2680 Woodlawn Drive, Honolulu, HI 96822, USA*

The submillimetre extragalactic background light is comparable with or exceeds that of the optical and ultraviolet (UV) wavelength ranges, showing directly that much of the energy radiated by star formation and active galactic nuclei is moved to far-infrared wavelengths. However, it is only as this background at 850 μm has been resolved with direct submillimetre imaging that we have seen that it is largely created by a population of ultraluminous (or near-ultraluminous) infrared galaxies, which appear to lie at relatively high redshifts ($z > 1$). Mapping the redshift evolution of this major portion of universal star formation has been difficult because of the poor submillimetre spatial resolution, but this difficulty can be overcome by using extremely deep centimetre continuum radio observations to obtain precise astrometric information, since the bulk of the brighter submillimetre sources have detectable radio counterparts. With this precise position information available, we find that most of the submillimetre sources are extremely faint in the optical and near-infrared ($I \gg 24$ and $K = 21$–$22$) and inaccessible to optical spectroscopy. Rough photometric redshift estimates can be made from combined radio and submillimetre energy distributions. We shall refer to this procedure as millimetric redshift estimation to distinguish it from photometric estimators in the optical and near-infrared. These estimators place the bulk of the submillimetre population at $z = 1$–$3$, where it corresponds to the high-redshift tail of the faint centimetre radio population. While still preliminary, the results suggest that the submillimetre population appears to dominate the star formation in this redshift range by almost an order of magnitude over the mostly distinct populations selected in the optical/UV.

**Keywords: submillimetre imaging; redshift evolution; extragalactic background light**

## 1. Introduction

The cosmic far-infrared (FIR) and submillimetre (SMM) background, which is the cumulative rest-frame FIR emission from all objects lying beyond our Galaxy, has recently been detected by the FIRAS and DIRBE experiments on the COBE satellite (Puget *et al*. 1996; Guiderdoni *et al*. 1997; Schlegel *et al*. 1998; Fixsen *et al*. 1998; Hauser *et al*. 1998) and has been found to be comparable with the total unobscured emission at optical/UV wavelengths.† This result directly shows that much of the

† FIRAS, Far-Infrared Spectrograph; DIRBE, diffuse infrared background experiment; COBE, Cosmic Background Explorer.

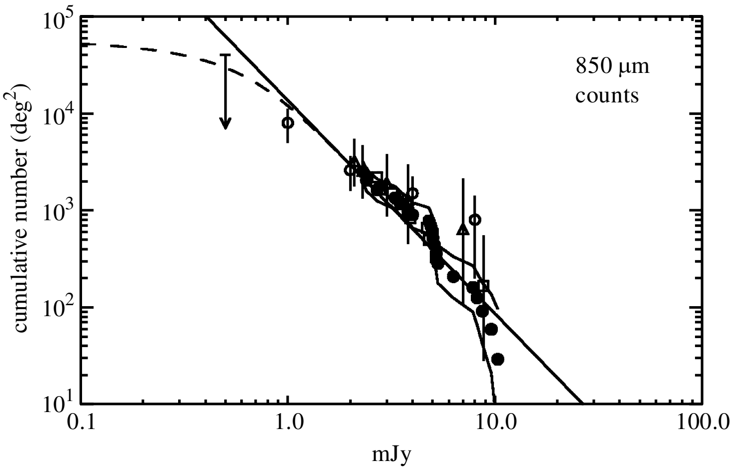


Figure 1. The 850 μm source counts from Barger *et al.* (1999*a–c*) (filled circles) with 1$\sigma$ error limits (jagged solid lines) are well described by the power-law parametrization in equation (2.1) with $a = 0.4$–$1.0$, $\alpha = 3.2$ and $N_0 = 3.0 \times 10^4\ \mathrm{deg}^{-2}\ \mathrm{mJy}^{-1}$ (solid line). The dashed curve shows a smooth extrapolation of this fit to match the EBL measurements using the value $a = 0.5$. Counts from Blain *et al.* (1999) (open circles), Hughes *et al.* (1998) (open triangles), and Eales *et al.* (1999) (open squares) are in good agreement with our data and the empirical fit.

energy released by the totality of star formation and active galactic nuclei (AGN) radiation through the lifetime of the Universe has been dust absorbed and reradiated into the rest-frame FIR. This, in turn, implies that to obtain a full accounting of the history of universal star formation, we must turn our attention to this dark side of the Universe.

## 2. Resolving the SMM background

The first stage in this process is to locate the individual objects that give rise to the background. Resolution of the extragalactic SMM background at 850 μm became possible almost simultaneously with the measurement of the background when the Submillimetre Common User Bolometer Array (SCUBA; see Holland *et al.* 1999) was installed on the 15 m James Clerk Maxwell Telescope (JCMT) on Mauna Kea. The SCUBA's sensitivity and area coverage enabled the sources producing the SMM background to be directly imaged for the first time. The current count determinations determined from blank-field surveys and from cluster-lensed fields (Smail *et al.* 1997; Barger *et al.* 1998, 1999*b*; Hughes *et al.* 1998; Blain *et al.* 1999; Eales *et al.* 1999) are shown in figure 1. Barger *et al.* (1999*a–c*) have shown, using optimal fitting techniques combined with Monte Carlo simulations of the completeness of the count determinations, that the cumulative counts are well fitted by a power law above 2 mJy. In addition, they showed that, in order to match the background and fit to the very limited information at fainter magnitudes from the lensed sample (Blain *et al.* 1999), a differential source count law

$$n(S) = N_0/(a + S^{3.2}), \tag{2.1}$$

was reasonable. Here, $S$ is the flux in mJy, $N_0 = 3.0 \times 10^4\ \mathrm{deg}^{-2}\ \mathrm{mJy}^{-1}$, and $a = 0.4$–$1.0$ is chosen to match the 850 μm extragalactic background light (EBL). The

95% confidence range for the power-law index is from 2.6 to 3.9. The extrapolation suggests that the typical SMM source producing the bulk of the background lies at around 1 mJy, and the direct counts show that *ca.* 30% of the 850 μm background comes from $N_0 = 3.0 \times 10^4\ \mathrm{deg}^{-2}\ \mathrm{mJy}^{-1}$, and $a = 0.4$–$1.0$ is chosen to match the 850 μm EBL. The 95% confidence range for the power-law index is from 2.6 to 3.9. The extrapolation suggests that the typical SMM source producing the bulk of the background lies at around 1 mJy, and the direct counts show that *ca.* 30% of the 850 μm background comes from sources above 2 mJy.

Provided only that the redshifts lie near or above $z = 1$ (see below), the FIR luminosity is approximately independent of the redshift. Thus, if we assume an ARP 220-like spectrum with $T = 47$ K (see, for example, Barger *et al.* 1998), the FIR luminosity of a characteristic *ca.* 1 mJy source is in the range $4$–$5 \times 10^{11} h_{65}^{-2} L_\odot$ for a $q_0 = 0.5$ cosmology ($7$–$15 \times 10^{11}$ for $q_0 = 0.02$). The FIR luminosity provides a measure of the current star-formation rate (SFR) of massive stars (Scoville & Young 1983; Thronson & Telesco 1986), $\mathrm{SFR} \sim 1.5 \times 10^{-10}(L_{\mathrm{FIR}}/L_\odot)M_\odot\ \mathrm{yr}^{-1}$; a 1 mJy source would, therefore, have an SFR of *ca.* $70 h_{65}^{-2} M_\odot\ \mathrm{yr}^{-1}$ for $q_0 = 0.5$, placing the 'typical' SMM source at or above the high end of extinction-corrected SFRs in optically selected galaxies (Pettini *et al.* 1998). If we were to allow the dust temperature to go as low as 30 K, $L_{\mathrm{FIR}}$ and the corresponding SFR would be approximately four times smaller.

## 3. Direct attempts at a redshift distribution

The identification of the optical/near-IR counterparts to the SCUBA sources is made difficult by the uncertainty in the 850 μm SCUBA positions and by the intrinsic faintness of the counterparts. Barger *et al.* (1999*c*) presented a spectroscopic survey of possible optical counterparts to a flux-limited sample of galaxies selected from the 850 μm survey of massive lensing clusters by Smail *et al.* (1997, 1998). The advantage of a lensed survey is that the clusters magnify any background sources, thereby providing otherwise unachievable sensitivity in detecting SMM sources, and easing spectroscopic follow-up in the optical. In the Barger *et al.* (1999*c*) survey, identifications were attempted for all objects in the SCUBA error boxes that were bright enough for reliable spectroscopy; redshifts or limits were obtained for 24 possible counterparts to a complete sample of 16 SCUBA sources. The redshift survey produced reliable identifications for six of the SMM sources: two high-redshift galaxy pairs (a $z = 2.8$ AGN/starburst pair (Ivison *et al.* 1998) and a $z = 2.6$ Lyman-break-like pair (Ivison *et al.* 2000); two galaxies showing AGN signatures ($z = 1.16$ and $z = 1.06$); and two cD galaxies (cluster contamination). The galaxy pairs were later confirmed as the true counterparts through the detection at their redshifts of CO emission at millimetre wavelengths (Frayer *et al.* 1998, 1999). Because AGN are very uncommon in optically selected spectroscopic samples, it is also probable that the AGN identifications are correct, and they place a rough lower limit of *ca.* 20% on the fraction of the SMM sources that have AGN characteristics. These results suggest that, excluding the cluster objects, about one-quarter of the SMM sources can be spectroscopically identified.

However, two of the SMM sources in the sample have no counterparts to $I$ around 26, and, while the remaining eight sources have optical galaxies within the large error circles, these are rather normal objects that may simply be chance projections. We

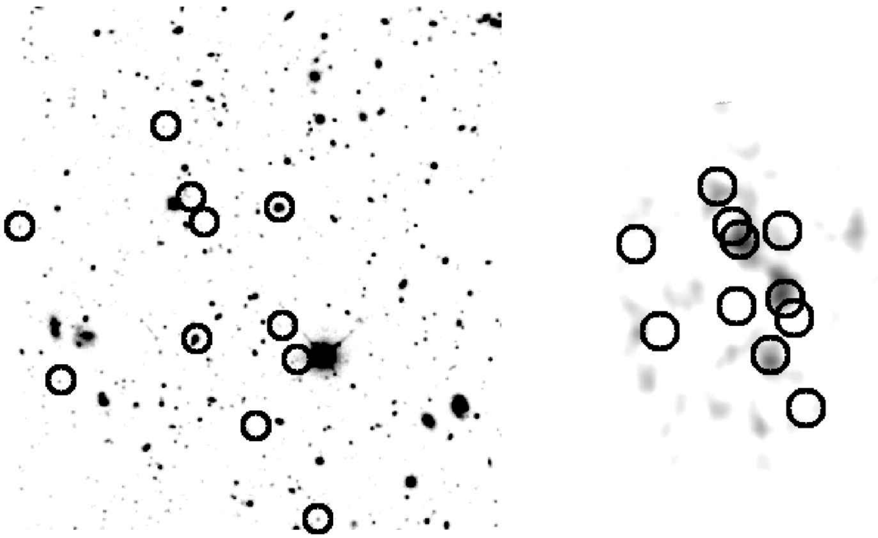

Figure 2. Radio sources in the HFF: the figure shows an overlay of the 20 cm radio sources in a small region of the HFF on a SCUBA 850 μm image on the right, and on a near-IR image of the region on the left. (North is to the right and east is to the top in these images.) In general, it is the radio sources that are faint in the optical and near-IR that are detected in the SMM.

shall show in the next section that this is very probably the case. These missing sources may be at higher redshifts, or be more dust obscured, than the spectroscopically identifiable sources. Furthermore, Smail *et al.* (1999), using deep near-IR and optical imaging of the fields, recently detected two extremely red objects that may be the counterparts of two of these sources, rather than the nearby bright spiral galaxies which Barger *et al.* (1999*c*) observed as the most likely counterparts to the SMM sources. This result also suggests that many of the optical source identifications may be suspect.

## 4. Positional determination from centimetre continuum radio observations

To proceed further we need accurate astrometric positions, and these are most easily obtained using centimetre radio continuum observations. Because of the well-known radio–FIR correlation, both the centimetre data and the SMM observations are linearly dependent on the SFRs in the galaxy (Condon 1992), though the ratio of the 850 μm flux to the centimetre radio flux rises rapidly as a function of redshift because of the opposite signs of the $K$-correction in the two wavelength ranges. (We discuss this further in the next section.) Because of the redshift dependence, a centimetre flux-limited sample will contain a high proportion of lower redshift objects, while the 850 μm sample will pick out primarily the high-redshift objects.

The flanking field region of the Hubble deep field (the Hubble flanking field (HFF)) is well suited to looking at the radio versus SMM selection. Richards (1999) recently obtained an extremely deep Very Large Aarray 20 cm image of this region, with a relatively uniform ($1\sigma = 8$ μJy) sensitivity over the whole flanking field region, which can be combined with the deep ground-based optical and near-IR (NIR) imaging of the HFF (Barger *et al.* 1999*a*). Richards *et al.* (1999) found that roughly two-thirds of the $5\sigma$-selected 20 cm population have relatively bright optical/NIR counterparts, while the remaining third are very faint. Barger *et al.* (1999*a*–*c*) observed a complete subsample of the radio-selected objects with the Low Resolution Imager and Spectrograph on the Keck II 10 m telescope, and found that nearly all the objects with $K < 20$ could be spectroscopically identified, with a maximum redshift of around 1.2; however, almost none of the fainter objects were identified.

From a total sample of 70 radio-selected galaxies in the HFF region, Barger *et al.* (2000) chose the 16 with $K > 21$ for follow-up with the SCUBA. However, because they used the jiggle map mode, which provides a *ca.* 5 arcmin$^2$ field around the target, a large fraction of the remaining radio sources (35/54) were also serendipitously measured. Fourteen of the 16 targeted blank-field sources were observed. Even with relatively shallow SCUBA observations ($3\sigma = 6$ mJy at 850 μm), a very large fraction of the blank-field radio sources were detected in the SMM, as is illustrated in figure 2. Of the 14 targeted sources, five are detected above 6 mJy, while, in contrast, none of the 35 optical/NIR bright sources were detected. In the observed fields, which covered slightly more than half of the HFF, a further two sources brighter than 6 mJy were discovered that were not in the radio sample. Even if there are further non-radio-detected SMM sources at the same level in the remaining unobserved portions of the HFF, it appears that the radio selection is turning up the majority of the bright SMM sources.

The fact that many of the bright SMM sources can be identified with the optical/NIR faint radio sources in this way has the extremely important corollary that many of the 850 μm selected sources have extremely faint optical/NIR counterparts. This is illustrated in figure 3, where we show the $K$ and $I$ magnitudes of radio-selected sources in the HFF, and also in the SSA13 field (see Richards *et al.* (1999) and references cited therein), where a similar SMM survey has been carried out (Cowie *et al.* 2000). Extremely deep $K$ observations with the near-IR camera on the Keck I 10 m can yield detections of nearly all the 850 μm detected radio sources, and these are found to lie in the $K = 21$–22 range. However, many of the sources are not detected in the $I$ band at the $2\sigma$ limit of $I = 25$ for the HFF, and, for the HDF850.2 source in the HDF proper (Hughes *et al.* 1998), the source is not seen to $I = 29$. The brightest sources lie in the $I = 24$–25 range.

## 5. Millimetric redshift estimation

While it is clear from the work described in § 3 that a fraction of the SMM sources have optical and NIR counterparts that are bright enough for spectroscopic identification, the results of § 4 show that a very large fraction simply cannot be identified in this way. At the current time, the small numbers of objects suggest that perhaps one-quarter of the sources (of which a fairly large fraction have AGN characteristics) are bright in the optical and spectroscopically identifiable category, while the remainder fall into the optical/NIR faint category. For this latter category of objects, we will have to rely on photometric estimates using the shape of the spectral energy distribution between radio and SMM wavelengths, and the SMM to NIR ratios (Carilli & Yun 1999; Blain *et al.* 1999).

Carilli & Yun (1999) have suggested the use of the 850 μm to 20 cm flux ratio as a redshift indicator. Because of the opposing spectral slopes of the synchrotron

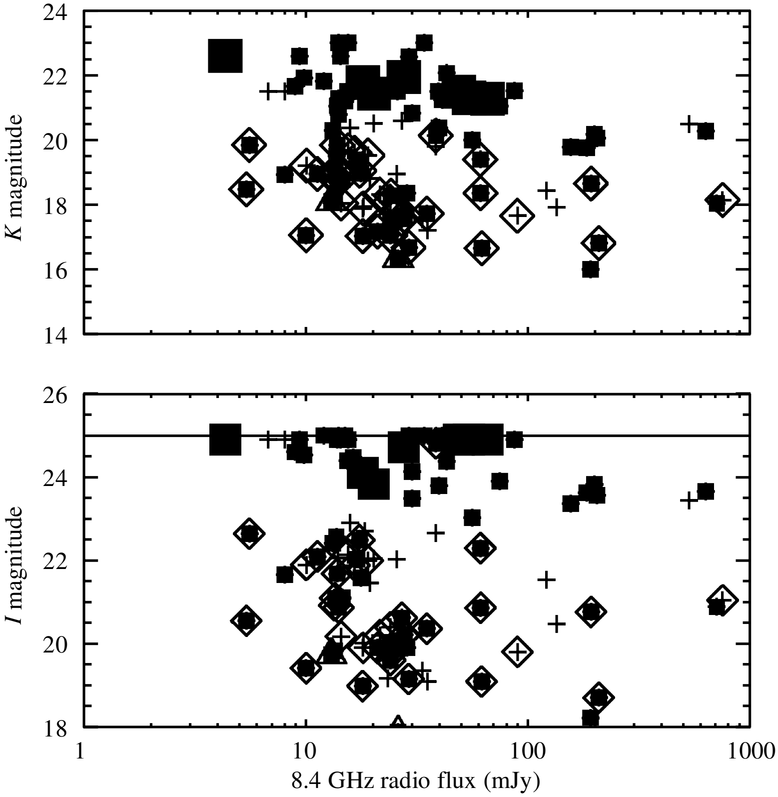


Figure 3. The optical and NIR magnitudes of the radio sources in the HFF and the SSA13 field versus 8.4 GHz flux: the whole radio population is shown as crosses with sources that only have 20 cm fluxes extrapolated to 8.4 GHz assuming a synchrotron spectrum. Sources with known redshifts are shown with open diamonds and all lie at $z < 1.2$, except for two quasars in the SSA13 field (Windhorst *et al.* 1995), which are shown as triangles. Sources that have been observed at 850 μm, but not detected at the typical 6 mJy ($3\sigma$) level, are shown as small squares, while those detected at 850 μm are shown as large squares.

spectrum in the radio and the black-body spectrum in the SMM, the SMM-to-radio ratio rises extremely rapidly with redshift, as is shown in figure 4 (which is taken from Barger *et al.* (1999*a*–*c*) in which a much more extensive discussion may be found). The primary uncertainty in this quantity lies in the dust temperature dependence, which, in the local ultraluminous IR galaxy (ULIG) sample, produces a range in the ratio of approximately a multiplicative factor of two relative to ARP 220.

We can test the estimator in a variety of ways. In figure 4 we have shown the average SMM-to-radio ratios for the objects in the HFF with known spectroscopic redshifts. While none of these sources is individually detected, the average values are consistent with a null result at low redshifts and a strongly significant positive detection for the sources near $z = 1$, which is extremely consistent with the ARP 220 ratio. Individual SMM sources with spectroscopic identifications are also broadly consistent with the expected ratios, though there is a suggestion that, as might be expected, those with the AGN characteristics have slightly lower ratios, though still within the broad general range.

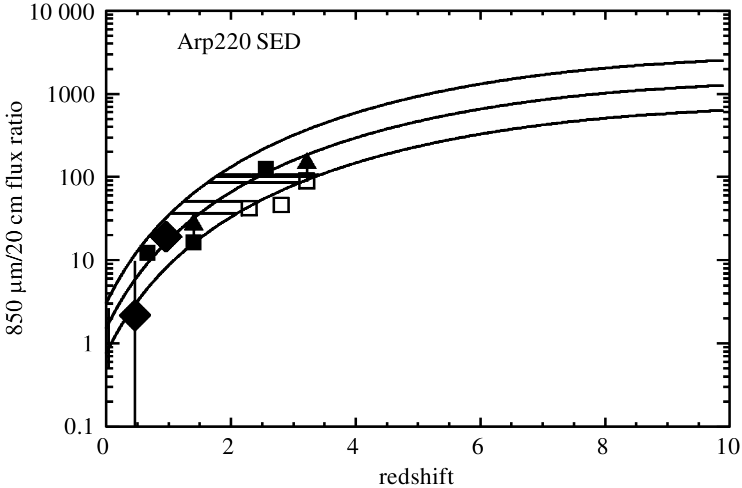


Figure 4. Millimetric redshift estimation: the solid curve shows the ratio of the 850 μm to 20 cm flux that a non-evolving ARP 220 would have as a function of redshift. The solid bar at low redshift shows the range of the 850 μm fluxes to the 8.4 GHz flux at low redshift extrapolated to 20 cm, assuming a synchrotron spectrum with the data taken from Rigopoulou *et al*. (1996). This suggests that the ULIGs have a range of about a multiplicative factor of two relative to ARP 220, which is shown by the dashed lines. The average SMM to 20 cm ratio of the galaxies that have spectroscopic redshifts and have also been observed in the SMM are shown as the large diamonds with $1\sigma$ errors. The lowest point is consistent with a null detection, but, in the higher redshift bin, there is a strong positive detection consistent with an ARP 220 ratio. Individually detected objects from Lilly *et al*. (1999) and Ivison *et al*. (2000) are also consistent within the error spread, although those with AGN characteristics (open symbols) appear to fall low in the figure. The solid line shows the best guess for the redshift range (typically $z = 1$–3) for the optically/NIR faint galaxies that are detected in the SMM. Radio objects that are not detected in the SMM are likely to lie at lower redshifts than this, while SMM-detected objects that are not seen in the radio are potentially at higher redshift.

The radio sources in the HFF, which are faint in the optical and NIR and which have some SMM detections are shown as the horizontal lines in the figure. The redshift estimator places them in the same broad, general, $z = 1$–3, range as the typical spectroscopically identified sources. (For AGN, we may be systematically underestimating the redshifts). Radio sources without 850 μm detections probably lie at lower redshifts, while the 850 μm sources without radio counterparts may represent the high-end redshift tail.

## 6. Conclusion

We can summarize the results as follows. Approximately 30% of the 850 μm background is already resolved and the slope of the counts is sufficiently steep (a power-law index of −2.2 for the cumulative counts) that only a small extrapolation to fainter fluxes will result in convergence to the background. Thus, the typical SMM source contributing to the background seems to be in the 1–2 mJy range. Because of the direct correspondence between flux and luminosity at these wavelengths we may identify the sources with ULIGs or near-ULIGs. About one-quarter of the sources have optical counterparts that are bright enough to be spectroscopically identified, and a large fraction of these show AGN characteristics, though at least one is an extremely bright pair of Lyman-break galaxies. However, many of the remaining sources are extremely faint at optical and NIR wavelengths ($K = 21$–$22$). Redshift estimation for these sources using the SMM-to-radio ratios places the bulk of them in the same, $z = 1$–$3$, range as the spectroscopically identified sources.

It is interesting to consider where this population fits into the overall history of universal star formation. One uncertainty in doing this is the question of what fraction of the SMM light is powered by AGN rather than star formation. It has long been debated whether the dust-enshrouded local ULIGs are powered by massive bursts of star formation induced by violent galaxy–galaxy collisions or by AGN activity. A recent mid-IR spectroscopic survey of 15 ULIGs by Genzel *et al*. (1998) found that 70–80% of the samples are predominantly powered by star formation and 20–30% by a central AGN. Thus, while the spectroscopic follow-up studies of the gravitationally lensed SMM sample (Barger *et al*. 1999*c*; Ivison *et al*. 1998) discussed in § 3 indicate that at least 20% of the sample show some AGN activity, we shall assume, in the following discussion, that a substantial fraction of the SMM light arises from star formation.

Several groups (Smail *et al*. 1998; Eales *et al*. 1999; Lilly *et al*. 1999; Trentham *et al*. 1999; Barger *et al*. 1999*a–c*) have suggested that the SMM sources are associated with major merger events giving rise to the formation of spheroidal galaxies. The approximate equality of the optical and SMM backgrounds supports this hypothesis; present-day spheroidal and disk populations have roughly comparable amounts of metal density, and, thus, their formation is expected to produce comparable amounts of light (Cowie 1988). Since the volume density of local ULIGs is very low (*ca.* $10^{-6}h_{65}^{3}$ Mpc$^{-3}$ for objects with bolometric luminosities above $5 \times 10^{11}h_{65}^{-2}L_{\odot}$; see, for example, Sanders & Mirabel (1996)), it appears that the SFR in this population must have been much higher in the past and must have declined very steeply after $z = 1$, which may also be consistent with this interpretation. For a cumulative source density of $4.0 \times 10^{4}$ deg$^{-2}$, required to reproduce the EBL with 1 mJy sources ($\langle N\rangle = \mathrm{EBL}/\langle S\rangle$ with $\langle S\rangle \sim 1$ mJy), and redshifts in the 1–3 range, the average space density is $5 \times 10^{-3}h_{65}^{3}$ Mpc$^{-3}$ for a $q_0 = 0.5$ cosmology ($10^{-3}$ for $q_0 = 0.02$). This space density is rather insensitive to the upper cut-off on the redshift distribution, dropping by only a factor of around 2 or 3 if we extend the volume calculation to $z = 5$. For comparison, the space density of present-day ellipticals is *ca.* $10^{-3}h_{65}^{3}$ Mpc$^{-3}$ (Marzke *et al*. 1994). Within the still-substantial uncertainty posed by the dust temperatures, the estimated SFR from SMM sources in the $z = 1$–$3$ range is *ca.* $0.3h_{65}M_{\odot}$ yr$^{-1}$ Mpc$^{-3}$ for $q_0 = 0.5$, which is nearly an order of magnitude higher than that observed in the optical range, *ca.* $0.04h_{65}M_{\odot}$ yr$^{-1}$ Mpc$^{-3}$ (see, for example, Steidel *et al*. 1999), suggesting that it is the SMM light that marks the bulk of the star formation at these redshifts.

We thank our collaborators Eric Richards, Dave Sanders, Ian Smail, Rob Ivison, Andrew Blain and Jean-Paul Kneib.

## References

Barger, A. J., Cowie, L. L., Sanders, D. B., Fulton, E., Taniguchi, Y., Sato, Y., Kawara, K. & Okuda, H. 1998 *Nature* **394**, 248.

Barger, A. J., Cowie, L. L., Trentham, N., Fulton, E., Hu, E. M., Songaila, A. & Hall, D. 1999*a* *Astr. J.* **117**, 102.
Barger, A. J., Cowie, L. L. & Sanders, D. B. 1999*b* *Astrophys. J.* **518**, L5.
Barger, A. J., Cowie, L. L., Smail, I., Ivison, R. J., Blain, A. W. & Kneib, J.-P. 1999*c* *Astr. J.* **117**, 2656.
Barger, A. J., Cowie, L. L. & Richards, E. A. 2000 *Astr. J.* (In the press.)
Blain, A. W., Kneib, J.-P., Ivison, R. J. & Smail, I. 1999 *Astrophys. J.* **512**, L87.
Carilli, C. L. & Yun, M. S. 1999 *Astrophys. J.* **513**, L13.
Condon, J. J. 1992 *A. Rev. Astron. Astrophys.* **30**, 575.
Cowie, L. L. 1988 In *The post-recombination Universe* (ed. N. Kaiser & A. N. Lasenby). Dordrecht: Kluwer.
Cowie, L. L., Barger, A. J. & Richards, E. A. 2000 *Astr. J.* (In preparation.)
Eales, S. *et al*. 1999 *Astrophys. J.* **515**, 518.
Fixsen, D. J., Dwek, E., Mather, J. C., Bennett, C. L. & Shafer, R. A. 1998 *Astrophys. J.* **508**, 123.
Frayer, D. T., Ivison, R. J., Scoville, N. Z., Yun, M., Evans, A. S., Smail, I., Blain, A. W. & Kneib, J.-P. 1998 *Astrophys. J.* **506**, L7.
Frayer, D. T., Ivison, R. J., Scoville, N. Z., Evans, A. S., Yun, M., Smail, I., Barger, A. J., Blain, A. W. & Kneib, J.-P. 1999 *Astrophys. J.* **514**, 13L.
Genzel, R. *et al*. 1998 *Astrophys. J.* **498**, 579.
Guiderdoni, B., Bouchet, F. R., Puget, J.-L., Lagache, G. & Hivon, E. 1997 *Nature* **390**, 257.
Hauser, M. G. *et al*. 1998 *Astrophys. J.* **508**, 25.
Holland, W. S. *et al*. 1999 *Mon. Not. R. Astr. Soc.* **303**, 659.
Hughes, D. H. *et al*. 1998 *Nature* **394**, 241.
Ivison, R., Smail, I., Le Borgne, J.-F., Blain, A. W., Kneib, J.-P., Bézecourt, J., Kerr, T. H. & Davies, J. K. 1998 *Mon. Not. R. Astr. Soc.* **298**, 583.
Ivison, R. *et al*. 2000 *Mon. Not. R. Astr. Soc.* (In the press.)
Lilly, S. J. *et al*. 1999 *Astrophys. J.* **518**, 641.
Marzke, R. O., Geller, M. J., Huchra, J. P. & Corwin Jr, H. G. 1994 *Astr. J.* **108**, 437.
Pettini, M., Kellogg, M., Steidel, C. C., Dickinson, M., Adelberger, K. L. & Giavalisco, M. 1998 *Astrophys. J.* **508**, 539.
Puget, J.-L., Abergel, A., Bernard, J.-P., Boulanger, F., Burton, W. B., Desert, F.-X. & Hartmann, D. 1996 *Astron. Astrophys.* **308**, L5.
Richards, E. A. 1999 *Astrophys. J.* **513**, 9L.
Richards, E. A., Fomalont, E. B., Kellermann, K. I., Partridge, R. B., Windhorst, R. A., Cowie, L. L. & Barger, A. J. 1999 *Astrophys. J.* **526**, L73.
Rigopoulou, D., Lawrence, A. & Rowan-Robinson, M. 1996 *Mon. Not. R. Astr. Soc.* **278**, 1049.
Sanders, D. B. & Mirabel, I. F. 1996 *A. Rev. Astron. Astrophys.* **34**, 749.
Schlegel, D. J., Finkbeiner, D. P. & Davis, M. 1998 *Astrophys. J.* **500**, 525.
Scoville, N. & Young, J. S. 1983 *Astrophys. J.* **265**, 148.
Smail, I., Ivison, R. J. & Blain, A. W. 1997 *Astrophys. J.* **490**, L5.
Smail, I., Ivison, R. J., Blain, A. W. & Kneib, J.-P. 1998 *Astrophys. J.* **507**, L21.
Smail, I., Ivison, R. J., Kneib, J.-P., Cowie, L. L., Blain, A. W., Barger, A. J., Owen, F. N. & Morrison, G. E. 1999 *Mon. Not. R. Astr. Soc.* **308**, 1061.
Steidel, C. C., Adelberger, K. L., Giavalisco, M., Dickinson, M. & Pettini, M. 1999 *Astrophys. J.* **519**, 1.
Thronson, H. A. & Telesco, C. M. 1986 *Astrophys. J.* **311**, 98.
Trentham, N., Blain, A. W. & Goldader, J. 1999 *Mon. Not. R. Astr. Soc.* **305**, 61.
Windhorst, R. A., Fomalont, E. B., Kellermann, K. I., Partridge, R. B., Richards, E., Franklin, B. E., Pascarelle, S. M. & Griffiths, R. E. 1995 *Nature* **375**, 471.